Chapter 6

Dynamic light scattering studies of some lyotropic nematics doped with DNA molecules

6.1 Introduction

In recent times there has been a lot of interest in the study of properties of polymers dissolved in anisotropic environments. Some of the systems that have come under scrutiny are polymeric side chain liquid crystals [1],[2] and spherical polystyrene particles dissolved in thermotropic nematics. Doping of biologically important molecules like DNA into lyotropic liquid crystals leads to a rich variety of phases [3], [4]. There have been suggestions that such systems can be used for applications like drug delivery.

In this chapter, we describe our dynamic light scattering (DLS) experiments on lyotropic liquid crystals doped with DNA molecules of different lengths. A nematic lyotropic liquid crystal was chosen as the host medium since it provides an ideal anisotropic aqueous environment. We describe our experiments to investigate the effects of the DNA polymer on the viscoelastic modes of the lyotropic nematic liquid crystal.

6.2 Experimental

First of all it is necessary to have a homogeneous dispersion of the DNA molecules in the lyotropic host. We use a simple lyotropic system composed of Cesium-perfluoro-

octanoate (CsPFO) in water. A part of the, phase diagram of this system is shown in figure(6.1). For our experiments we prepared lyotropic samples with 45% CsPFO and 55% water. We used de-ionized bacteria free millipore water. The dashed line in the figure shows the phases of this sample at various temperatures on the phase diagram. The sample is in the lamellar phase at room temperature. On slightly increasing the temperature, the sample could be taken in a controlled fashion to the nematic and isotropic phases. Our samples were taken in flat glass capillaries that had a width of 4mm and an inner gap of $400\mu m$. The samples were heated close to their isotropic temperature and brought in contact with the glass capillary. Due to capillarity the sample gets drawn in. To prevent water evaporation, the capillary tube is flame sealed at both ends. The stock samples are stored in air tight containers. The transition temperatures were observed in a polarizing microscope. As the temperature was increased, characteristic focal conic texture of the lamellar phase was clearly seen giving way to the nematic characterized by its schlieren texture. The phase transition temperatures for our system are:

$$L_D \overset{29.2^\circ C}{\longleftrightarrow} N_D \overset{35.5^\circ C}{\longleftrightarrow} I$$

We find that the transition temperatures are very sensitive to concentration of CsPFO in water.

Homeotropic alignment (the director n is parallel to the cell normal) in the nematic phase was induced by cycling the sample across the nematic-isotropic transition temperature a few times.

6.2.1 Sample preparation and characterization

We dispersed several kinds of DNA molecules in the liquid crystalline host. All the DNA samples were procured commercially. The glassware and containers used to handle and store the DNA material were thoroughly sterilized before use to free them from bacteria that might cleave the DNA molecules. We found that DNA procured in its powder form from sources like calf thymus, herring sperm and salmon testes do not dissolve well in the CsPFO system. On dissolving higher concentrations of DNA

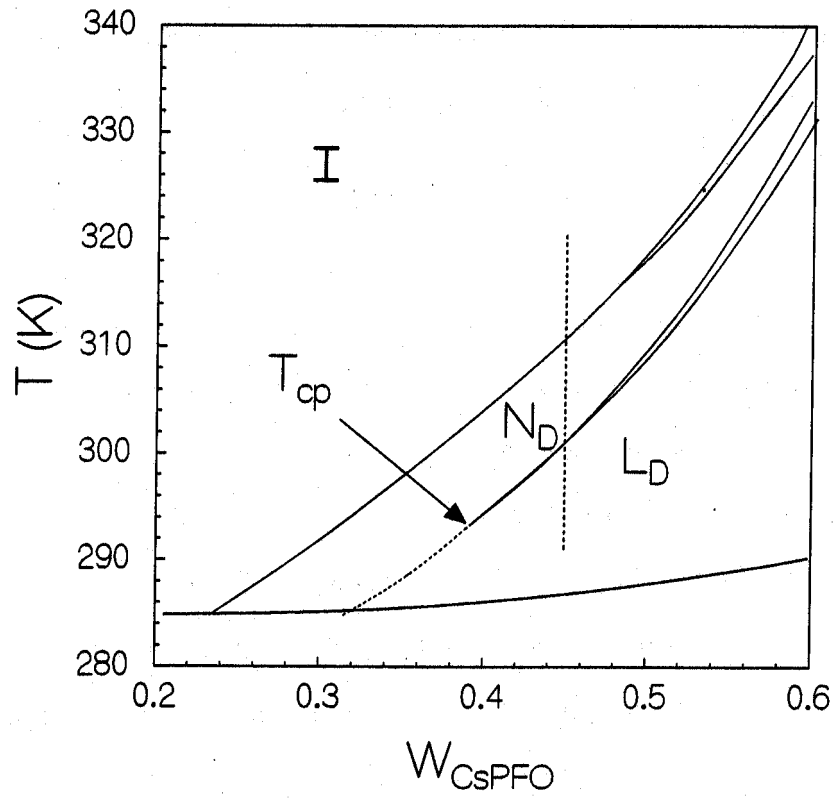

Figure 6.1: A partial phase diagram of the CsPFO/water system (after ref [5]). Here I is the isotropic phase, N_D is the discotic nematic phase and L_D is the discotic lamellar phase. The nematic to lamellar transition line ends in a critical point shown in the figure as T_{cp}. We have used a CsPFO/water concentration indicated by the dashed vertical line in the diagram. The dashed line in the figure shows the phases of this sample at various temperatures on the phase diagram.

molecules, they precipitated at the bottom of the container. At lower concentrations, inhomogeneities in the sample exist as observed under the polarizing microscope. On the other hand, we found that DNA of lower molecular weights procured in solution form dissolve more readily in the lyotropic system. We obtained two types of DNA supplied at high concentration in solution form. They are M13 DNA of 7.25 kilo base pairs (kbp) and the X DNA of 48.5 kilo base pairs. Both the types of DNA were suspended in 10mM Tris-HCL (pH 8) and 1mM EDTA solution. Here, EDTA acted as a chelating agent. It prevented stray enzymes from cleaving the DNA molecule. Various concentrations of the DNA solutions in water were prepared by diluting the stock solutions. The relation:

$$c_i\, v_i = c_f\, v_f$$

was used to determine the amount of water to be added to the known concentration of the stock solution to get a required concentration. In this relation c_i and c_f are the initial and final concentrations and v_i and v_f are initial and final volumes of the solvents. The lyotropic nematic was prepared directly with DNA solutions of various concentrations in the weight ratio 45% CsPFO and 55% DNA solution.

In order to check the state of fragmentation of the DNA molecules we performed horizontal agarose gel electrophoresis runs on our samples. The samples that were loaded in the gel were i) the pure M13 DNA, ii) the lyotropic-M13 DNA mixture where the M13 DNA concentration was 150μg/ml, iii) the pure X DNA, iv) the lyotropic-X DNA mixture where the λ DNA concentration was 125μg/ml and v) pure CsPFO.,Lane (vi) is the reference with X Hind III marker. The gel run was done with 70 volts applied across the gel for a duration of 1 hour. Our results are shown in figure(6.2). The bright sharp band in the pure M13 in lane, implies that most of the DNA molecules in the sample are of a single size. Three other faint bands corresponding to a small amount of lower molecular weight fragments can also be seen. In lane (ii) corresponding to the M13 doped lyotropic one can see a similar but slightly retarded band structure. In lane (iii) for pure λ DNA there is a single wide band. This implies that there is a distribution in the sizes of the XDNA molecules in

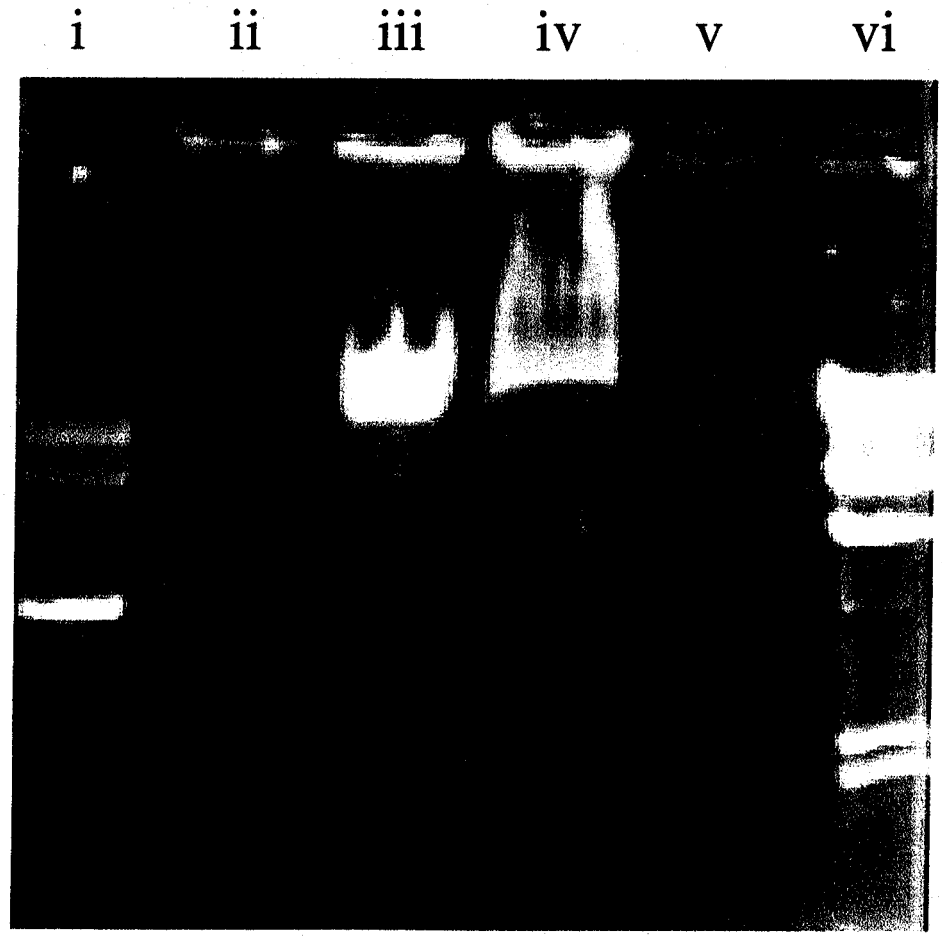

Figure 6.2: Results of the agarose gel run on the pure DNA samples and the lyotropic doped DNA samples. The samples loaded in the various lanes are i) Pure M13 DNA; ii) CsPFO + M13 DNA (150μg/ml); iii) pure λ DNA; iv)CsPFO + λ DNA (125μg/ml); v) pure CsPFO; vi) λ Hind III marker.

the sample. In lane (iv) corresponding to the lyptropic doped λ DNA a similar spread in the band is observed. The pure CsPFO, in lane (v), has no bands as expected. We also observe that the bands corresponding to the lyotropic doped DNA are uniformly retarded with respect to those of the pure DNA.

The gel electrophoresis run gave us a qualitative idea of the size distributions of the DNA molecules used in the experiments. Further, it confirmed that mixing the lyotropic with the DNA molecules did not drastically affect the lengths of the DNA molecules.

To check the optical homogeneity of the filled sample cells, several dynamic light scattering runs were performed on the same cell with the incident light illuminating different portions of the cell. The relaxation times obtained from different settings of the cell were identical within experimental errors. This confirmed the optical homogeneity of the sample.

6.2.2 The scattering arrangement and experimental details

The scattering arrangement employed by us is shown in figure(6.3). The incident light, from a 488 nm Argon ion laser, is polarized in a direction perpendicular to the scattering plane. Scattered light polarized in a direction parallel to the scattering plane is detected. This is the VH arrangement, where only the twist fluctuations of the director contribute to light scattering.

Here the cell was not immersed in a refractive index matching fluid. Hence, a correction had to be applied to the observed angle of scattering. The correction is the same as that given in chapter 3. The relation between the observed and the corrected angles is given by

$$\theta_{cor} = sin^{-1}\left(\frac{\mu_{air}}{\mu_{sample}} sin(\theta_{obs})\right) \tag{6.1}$$

Here, μ_{air} is the refractive index of air and μ_{sample} is the average refractive index of the sample. We measured the average refractive index of our lyotropic nematic samples using an Abbe refractometer (Carl Zeiss). The light source used in the Abbe refractometer had a wavelength comparable to the laser light used in the experiment.

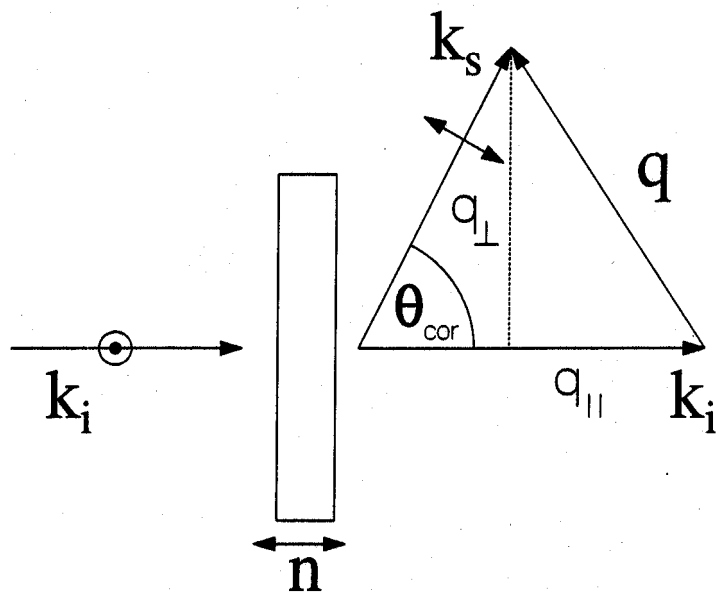

Figure **6.3: A** schematic diagram of the scattering arrangement used in the experiment. The sample is aligned homeotropically in the cell i.e., the director is parallel to the cell normal. In the geometry shown, pure twist fluctuations can be observed. $\mathbf{k_s}$ and $\mathbf{k_i}$ are the wavevectors of the scattered and incident beams. q is the scattering wavevector and θ_{cor} is the scattering angle. The directions of polarizations of the incident and scattered beams are in the V($\odot$) and H($\leftrightarrow$) arrangement respectively.

We found the value μ_{sample} to be equal to 1.4. The value of μ_{sample} of the lyotropic nematics doped with various concentrations of DNA molecules was practically the same.

The temperature control system and the oven used in our experiment have already been described in detail (chapters **2** and **3).** Here, we describe a modification that was made in the oven to accommodate the long flat glass capillaries used in this experiment. The glass capillaries could not be mounted on the holder. Instead a slot was made in the teflon jacket of the oven and the capillary was inserted through it such that the the sample was in the middle of the tunnel, in the path of the incident beam. The holder was slid through the tunnel till it came in firm contact with the flat wall of the capillary tube. **A** brass washer was pushed in from the other end of the tunnel till it came in contact with the opposite face of the capillary. The brass washer helped to prevent temperature gradients in the sample. The inner walls of the brass washer were made to taper radially outwards to avoid the obstruction of scattered light. The light scattered from the sample was detected by a photomultiplier tube (PMT). The signals from the PMT were suitably amplified by an amplifier discriminator system and passed on to a digital autocorrelator. These are described in detail in chapter **3.** Using this set up, correlograms for various angles and temperatures were obtained. For each sample, the intensity autocorrelation functions in the experiments were obtained at a temperature 2°C above its lamellar-nematic transition temperature.

6.2.3 Analysis of the intensity autocorrelation

In the experiments, the scattering arrangement was such that only twist fluctuations of the director contributed to the signal. Hence, all the intensity autocorrelation functions obtained in this experiment have a single exponential decay. We fit the intensity autocorrelation functions to a single exponential model of the type:

$$g_2(\tau) = u_1 + u_2 e^{-(\tau/u_3)}$$

Here u_1 is the base line parameter, u_2 is the strength of the decay and u_3 is the relaxation time.

We define the normalized autocorrelation function as:

$$G_2(\tau) = \frac{g_2(\tau)}{g_2(\infty)} - 1 = u_2' e^{-(\tau/u_3)}$$

Here, $u_2' = \frac{u_2}{g_2(\infty)}$. $g_2(\infty)$ is the base line. This value is automatically calculated by the correlator by using very long delay times. In figure(6.4) we show a typical normalized intensity autocorrelation function obtained for a nematic sample doped with $125\mu g/ml$ concentration of λ **DNA.**

In figure(6.5) we show a typical normalized intensity autocorrelation function obtained for a nematic sample doped with $150\mu g/ml$ concentration of **M13 DNA.**

From the intensity autocorrelation functions the relaxation time (τ) was determined. This experiment was carried out at various scattering angles. The plot of the inverse relaxation time as a function of the square of the scattering wavevector is given in figure(6.6). The slope of this curve gives the value of the viscoelastic coefficient.

6.3 Results and discussions

We carried out dynamic light scattering experiments for lyotropic nematics doped with **DNA** molecules. We measured the twist viscoelastic coefficient as a function of the concentration of **DNA** molecules in the nematic solvent. For comparison, we also determined the twist viscoelastic coefficient of pure CsPFO in its nematic phase. Our results are shown in figure(6.7). In the case of the low molecular weight **DNA** viz., the **M13 DNA** (7.5 kbp), the twist viscoelastic coefficient does not show any appreciable dependence on the concentration of the **DNA** molecules in the system. This is seen in the concentration range $75\mu g/ml$ to $300\mu g/ml$. In the case of the higher molecular weight λ **DNA** (48 kbp), the twist viscoelastic coefficient decreases with increasing concentration of **DNA** molecules in the system. The initial decrease is rapid, but at higher concentrations the viscoelastic ratio appears to saturate. The λ **DNA** concentration in these studies range from $31.25\mu g/ml$ to 250 $\mu g/ml$. These results are depicted in figure(6.7).

We interpret that the M13 **DNA,** being very small, disperse evenly in the system and

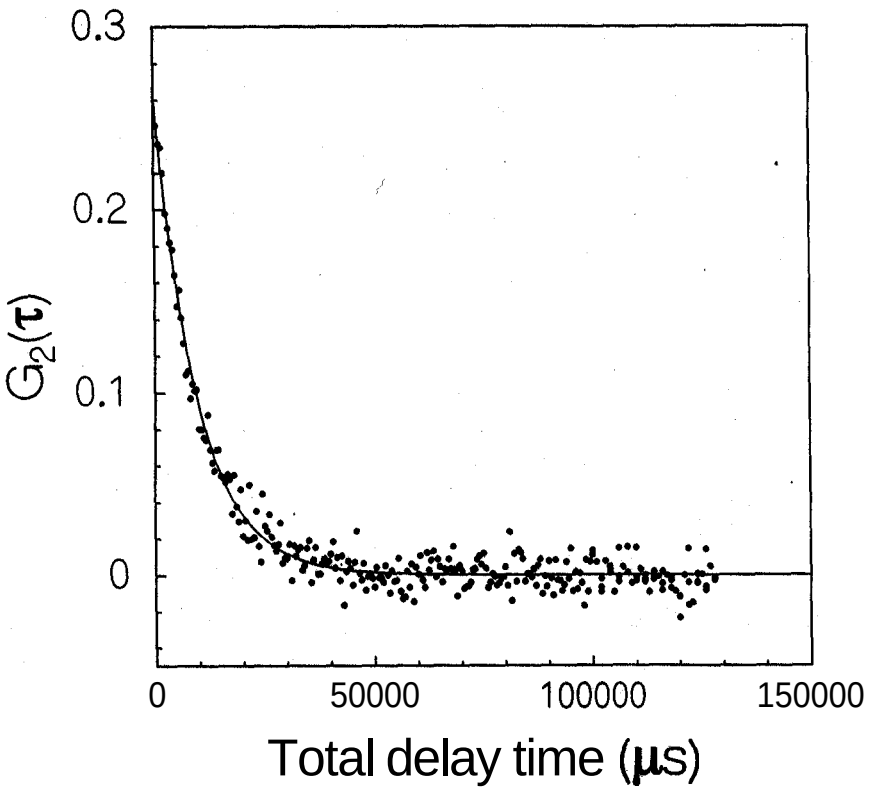

Figure 6.4: A typical normalized intensity autocorrelation function obtained for the nematic phase of CsPFO doped with molecules of λ DNA. The concentration of DNA molecules was $125\mu g/ml$. The corrected angle of scattering was 27.3 degrees. The correlator delay time was $500\mu s$ and the total integration time was 300 seconds. The sample temperature was maintained at $33 \pm 0.05°C$. The solid line shows a fit to a single exponential decay.

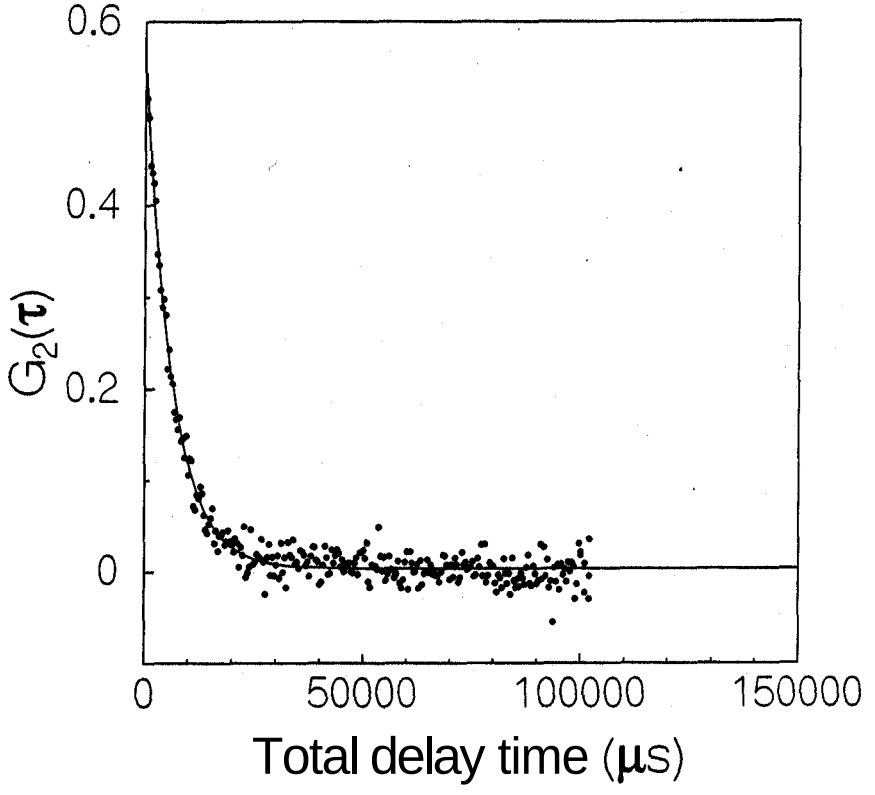

Figure 6.5: A typical normalized intensity autocorrelation function obtained from the nematic phase of CsPFO doped with molecules M13 DNA. The concentration of DNA molecules was $150\mu g/ml$. The angle of scattering, delay time and the total integration time were the same as that given in figure(6.4). The sample temperature was maintained at 32f 0.05°C. The solid line shows a fit to a single exponential decay.

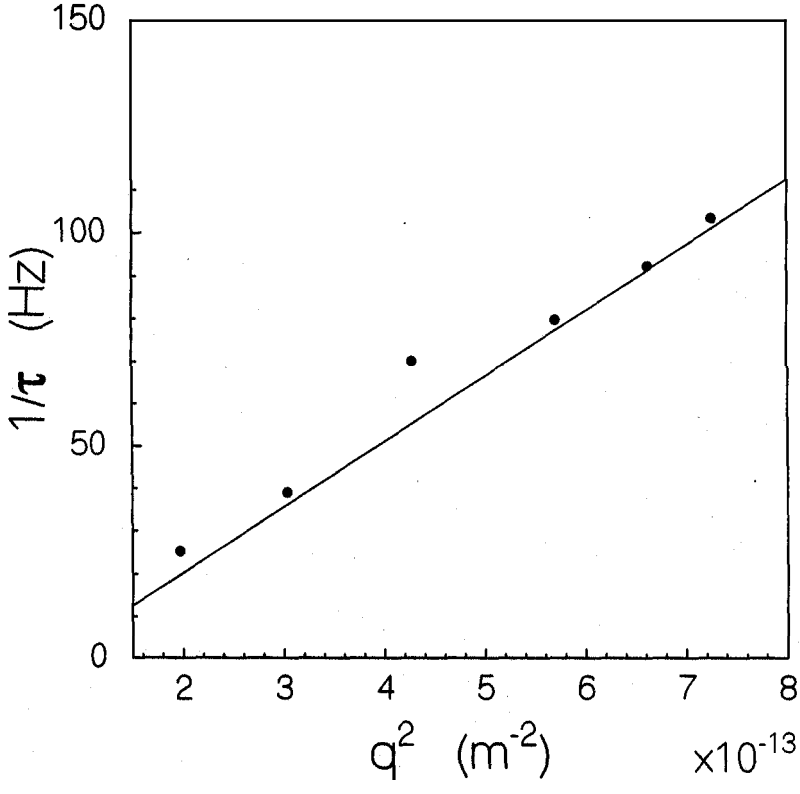

Figure 6.6: A plot of the inverse relaxation time as a function of the square of the scattering wavevector. The slope of the line gives the viscoelastic coefficient. The data shown was obtained for the nematic doped with λ DNA. The DNA concentration was $125\mu g/ml$. The sample temperature was maintained at 33f $0.05°C$. The solid line is a straight line fit to the data. The value of the twist viscoelastic coefficient obtained from this data is $1.54\times10^{-12}m^2/s$.

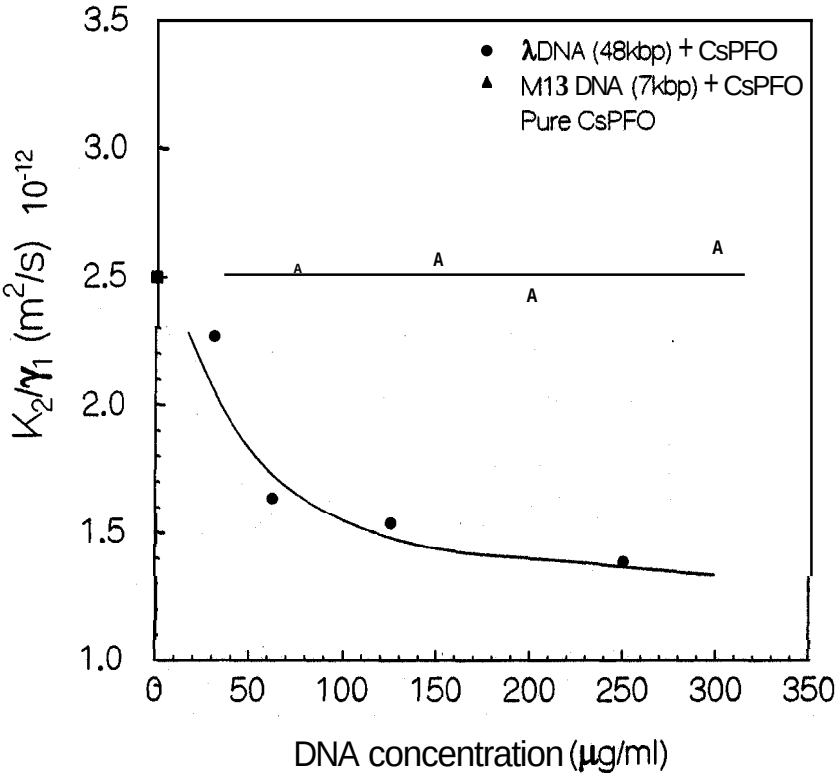

Figure **6.7:** Illustrating the effect of various concentrations of DNA molecules on the twist viscoelastic coefficient of the CsPFO nematic. i) For the λ DNA, indicated by filled circles, the twist viscoelastic coefficient decreases as the concentration of DNA molecules in the lyotropic nematic is increased. ii) For the **M13** DNA, indicated by the filled triangles, the twist viscoelastic coefficient is independent of the concentration of DNA molecules in the nematic solvent. iii) For comparison we have obtained the value of the twist viscoelastic coefficient of the pure CsPFO system and indicated it on the y axis as a filled square. The solid lines are drawn as a cue to the eye.

do not affect the modes of the director fluctuations in the host. On the other hand, the much longer λ **DNA** is likely to be in a spatially extended form and is able to affect the viscoelastic modes. **A** systematic study of differently sized **DNA** molecules may give an insight into the interactions and dynamics of **DNA** molecules in the nematic solvent. In addition to affecting the viscoelastic coefficients, the **DNA** molecules would also undergo diffusive Brownian motion in the lyotropic host material. But in our experiments we do not observe the relaxation times corresponding to the diffusion of **DNA** molecules. This might be due to the fact that the diffusive motion of the large **DNA** molecules is rather slow. Such slow movements will result in intensity fluctuations on large time scales. Fluctuations with such long time scales are out of the detection range of our present experimental set up.

The radius of gyration of polymers dissolved in solvents is a very sensitive function of concentration. In an anisotropic environment, as in a nematic liquid crystal, the shape of the compact **DNA** molecule might not even be spherical. The diffusion properties of non-spherical objects depends on the anisotropic structure of the host. **A** proper selection of DNA molecules matching the micellar size of the nematic solvent may bring out the anisotropic diffusion properties of the dissolved polymers.

More studies on relaxation times as a function of temperature in the nematic and lamellar phases are needed to be performed to get a better understanding of the behavior of such complex mixed systems.

Bibliography

[1] Pei-Yuan Liu, Ning Yao, and Alex M. Jamieson. Macromolecules, 32, 6587 (1999).

[2] D. F. Gu and A. M. Jamieson. Macromolecules, 27, 337 (1994).

[3] J. O. Radler, I. Koltover, T. Salditt, and C. R. Safinya. Science, 275, 810 (1997).

[4] T. Salditt, I. Koltover, J. O. Radler, and C. R. Safinya. Phys. Rev. Lett., 79, 2382 (1997).

[5] N. Boden, S. A. Corne, and K. W. Jolley. J. Phys. Chem., 91, 4092 (1987).